

DispVoxNets: Non-Rigid Point Set Alignment with Supervised Learning Proxies

Soshi Shimada^{1,2}

Vladislav Golyanik³

Edgar Tretschk³

Didier Stricker^{1,2}

Christian Theobalt³

¹University of Kaiserslautern

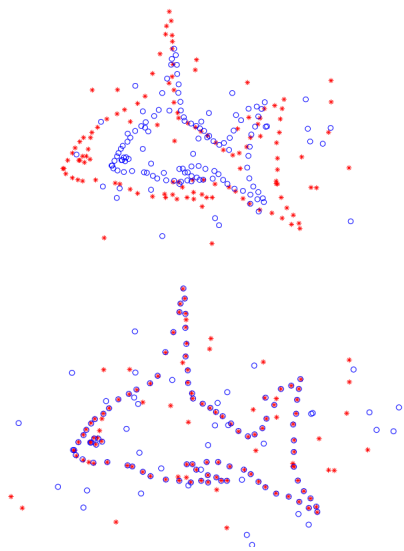
²DFKI

³MPI for Informatics, SIC

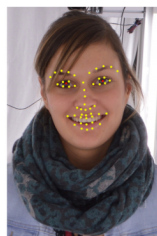


Non-rigid Point Set Registration (NRPSR)

Objective: given two point sets, find displacements (or correspondences) between the point sets.



2D point set registration
[Myronenko and Song 2010]



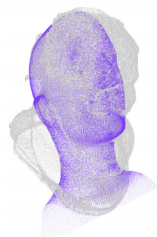
(a) frontal view



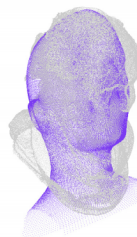
(b) mesh



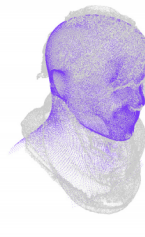
(c) template



(d) CPD, $w=0.1$

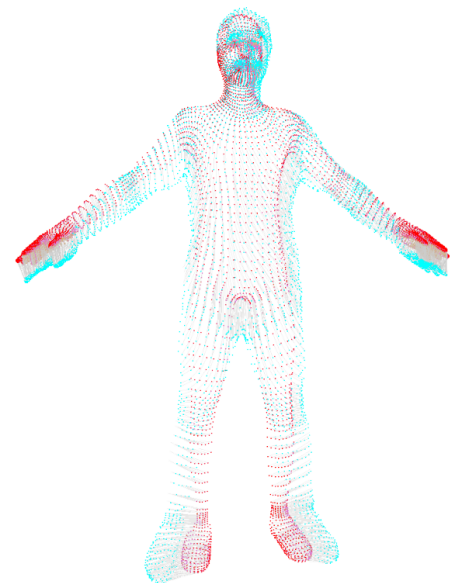


(e) CPD, $w=0.4$



(f) ECPD

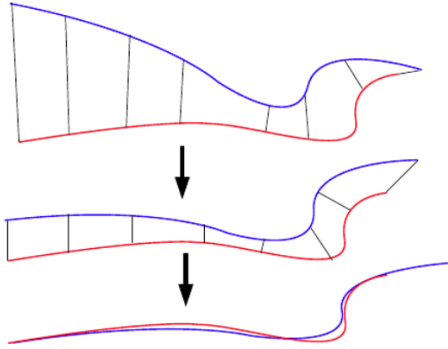
3D face registration
[Taetz *et al.* 2016]



3D pose registration
[Golyanik *et al.* 2017]

Related Works, General-Purpose Methods

Related Works, General-Purpose Methods

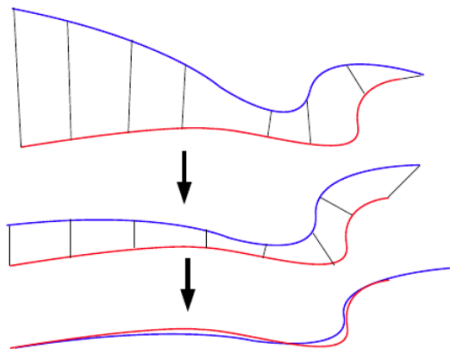


Iterative Closest Point (ICP)

[Besl and McKay 1992]

the image is taken from [Smistad *et al.* 2015]

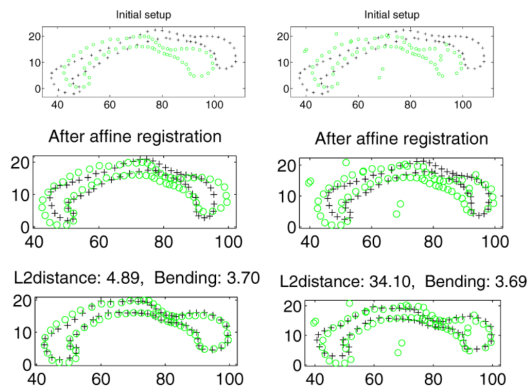
Related Works, General-Purpose Methods



Iterative Closest Point (ICP)

[Besl and McKay 1992]

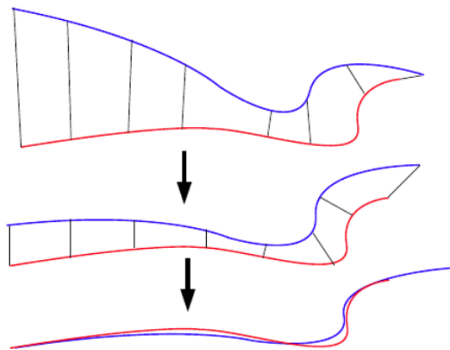
the image is taken from [Smistad *et al.* 2015]



Gaussian Mixture Model Registration (GMR)

[Jian *et al.* 2005]

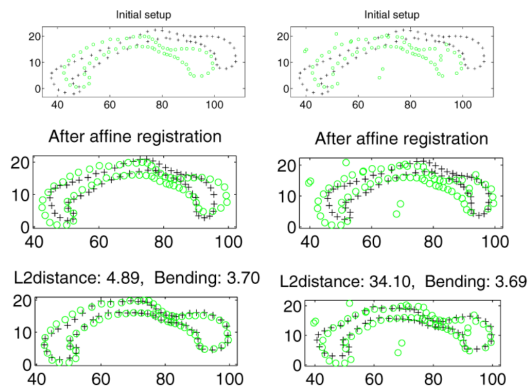
Related Works, General-Purpose Methods



Iterative Closest Point (ICP)

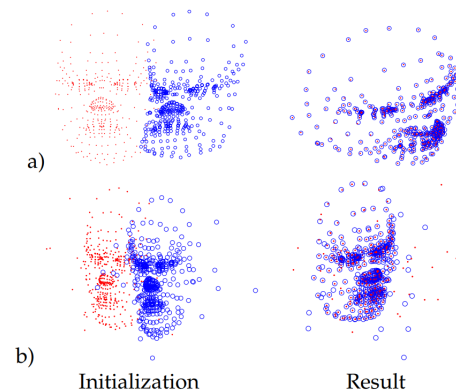
[Besl and McKay 1992]

the image is taken from [Smistad *et al.* 2015]



Gaussian Mixture Model Registration (GMR)

[Jian *et al.* 2005]

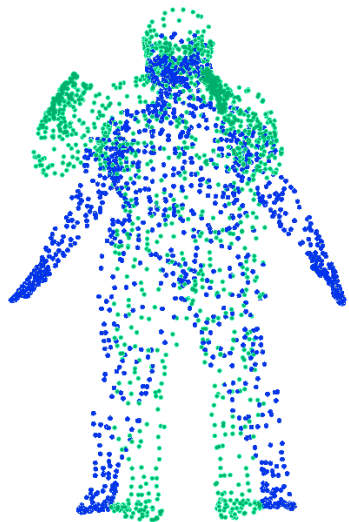


Coherent Point Drift (CPD)

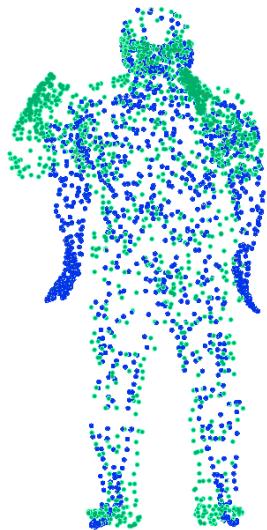
[Myronenko and Song 2010]

Related Works, General-Purpose Methods

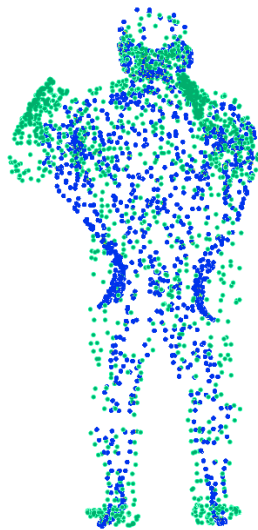
Green : reference
Blue : template



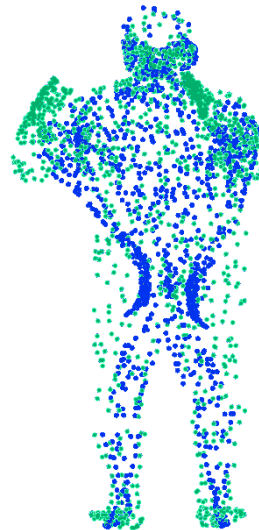
Initialisation



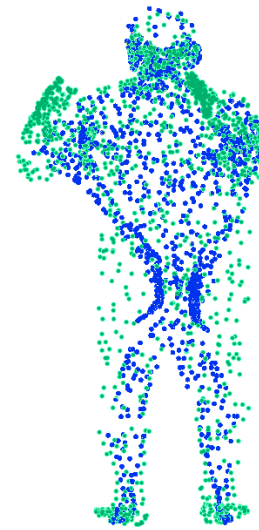
Iteration 25



Iteration 50



Iteration 75



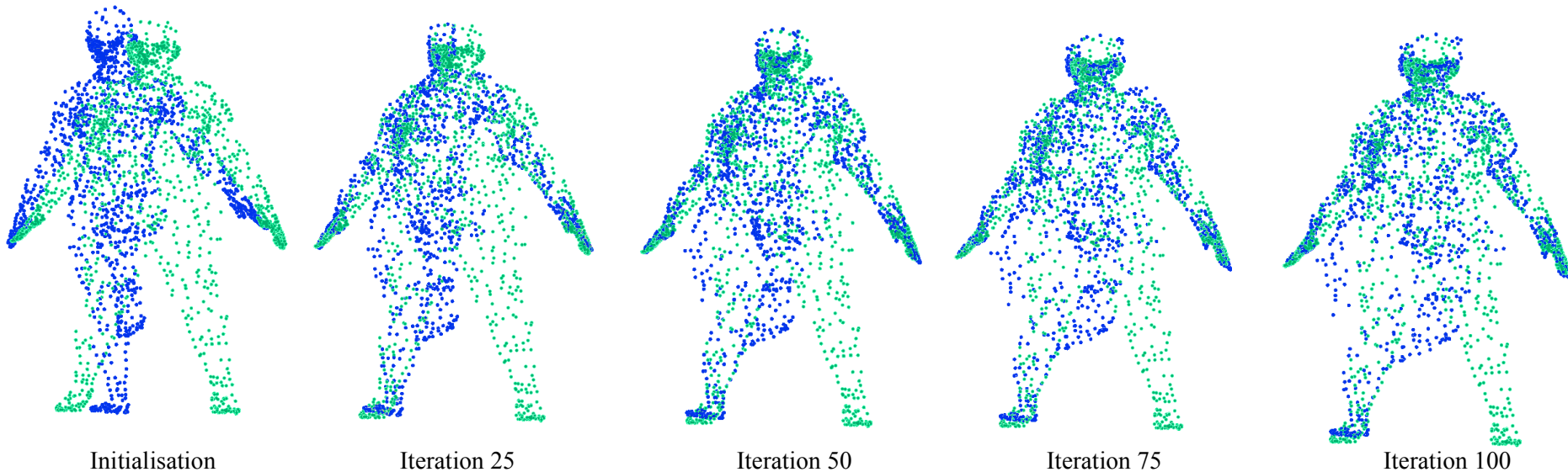
Iteration 100

Gravitational Approach for NRPSR

[Ali *et al.* 2018]

Related Works, General-Purpose Methods

Green : reference
Blue : template



Gravitational Approach for NRPSR

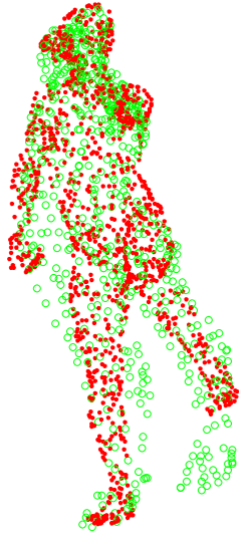
[Ali *et al.* 2018]

➔ Often fails with large deformations and articulated motions between the point sets.

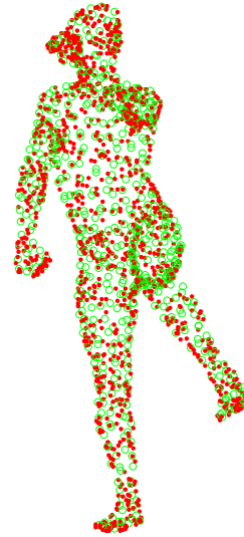
Related Works, General-Purpose Methods



Target



CPD

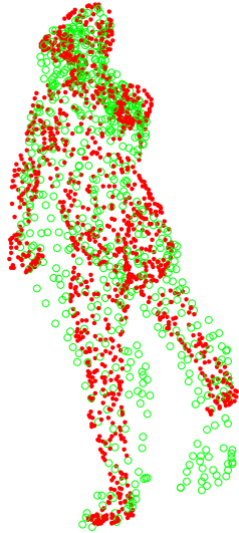


GLTP
[Ge *et al.* 2014]

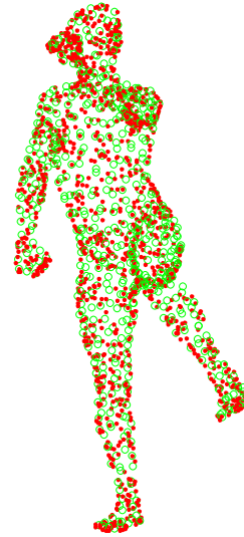
Related Works, General-Purpose Methods



Target



CPD



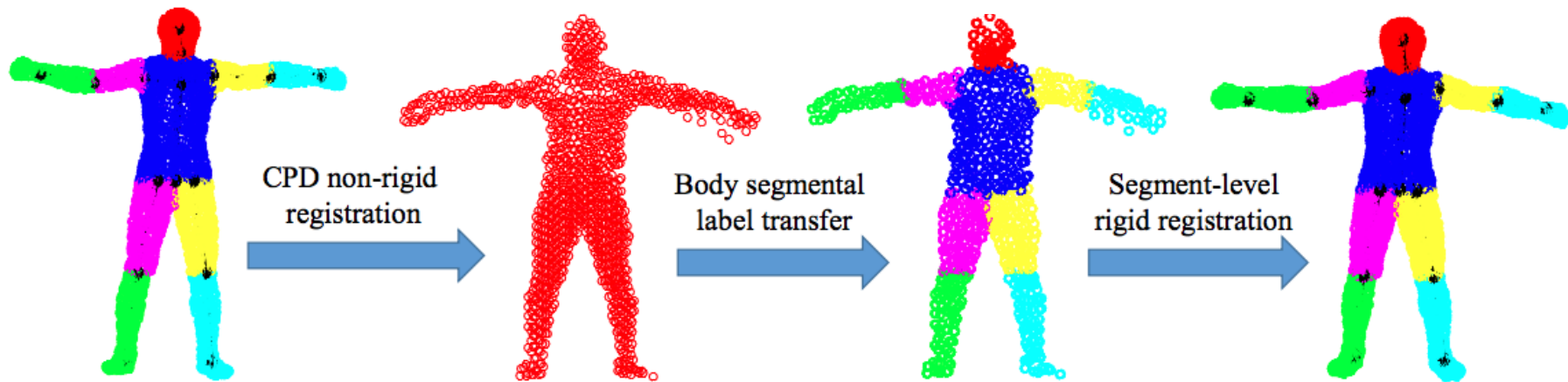
GLTP

[Ge *et al.* 2014]



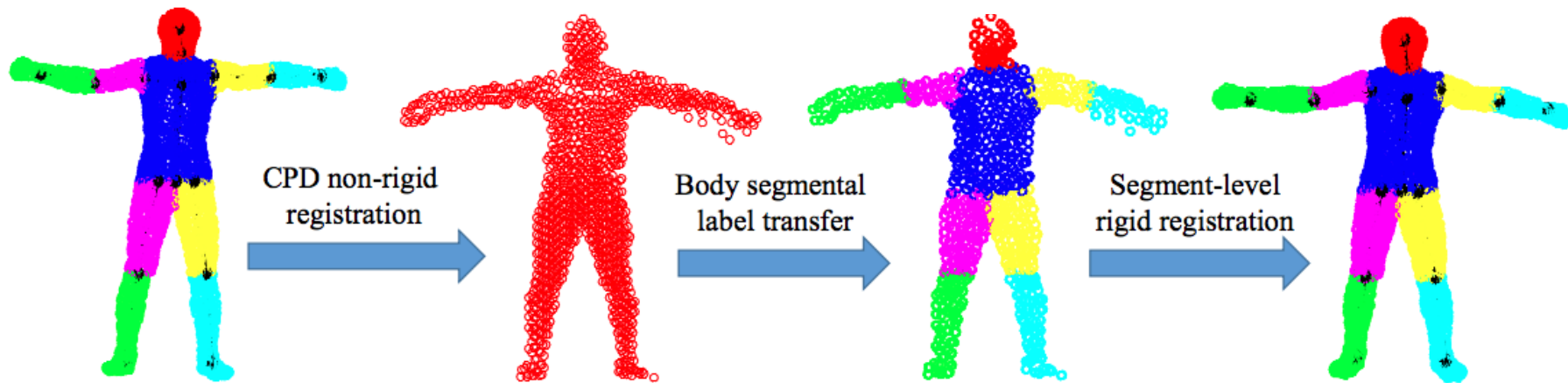
Relatively accurate however sensitive to noises

Related Works, Class-Specific Methods



[Ge and Fan 2015]

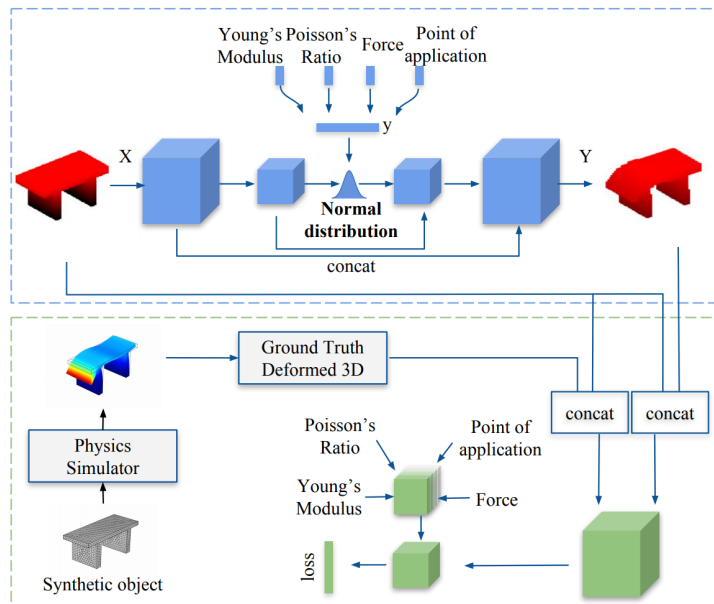
Related Works, Class-Specific Methods



[Ge and Fan 2015]

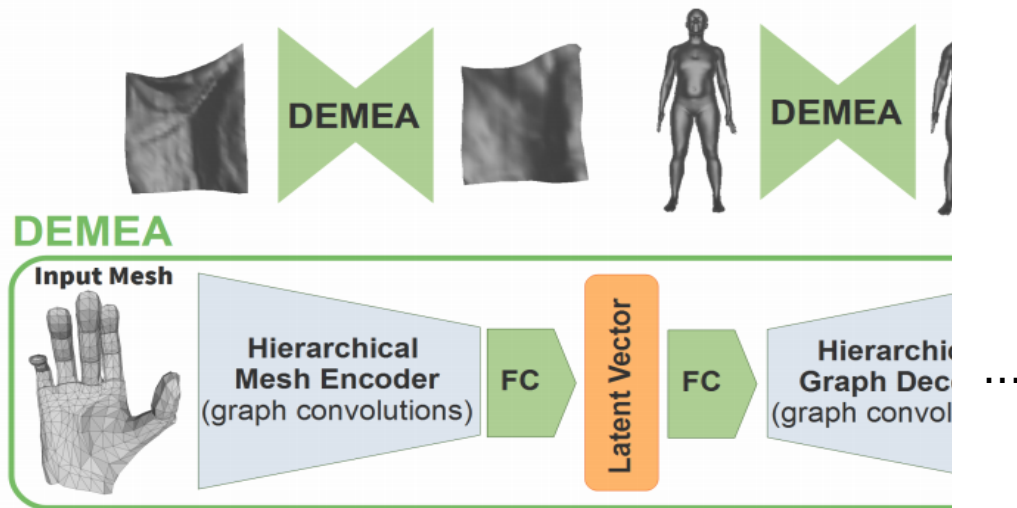
➔ Perform well with large deformations and articulated motions between the point sets.
However, the generalisability is limited.

Related Works, Neural Network Based Approaches (Other Fields)



3D-PhysNet

[Wang *et al.* 2018]

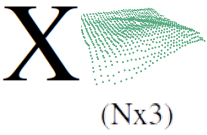
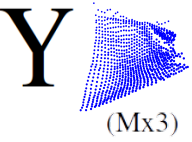


DEMEA

[Tretschk *et al.* 2019]

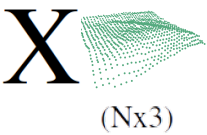
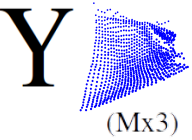
Pipeline

Pipeline



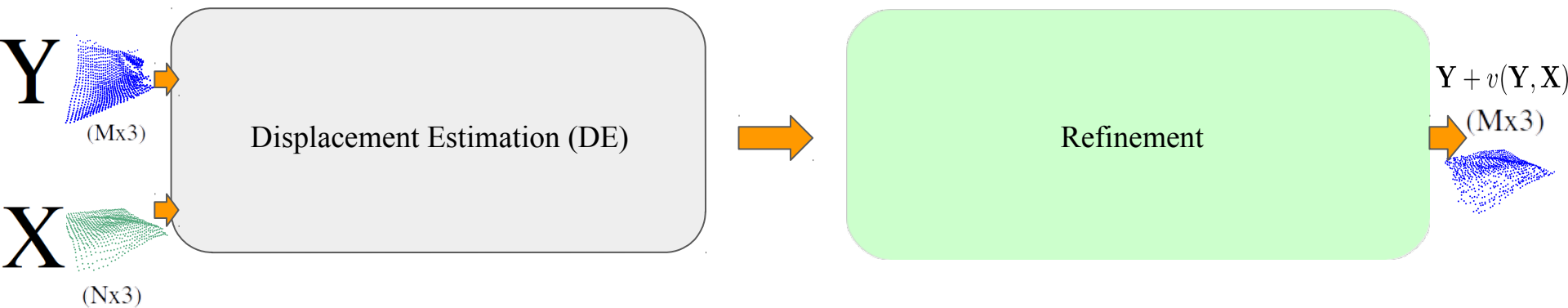
- Y: template point set, X: reference point set

Pipeline



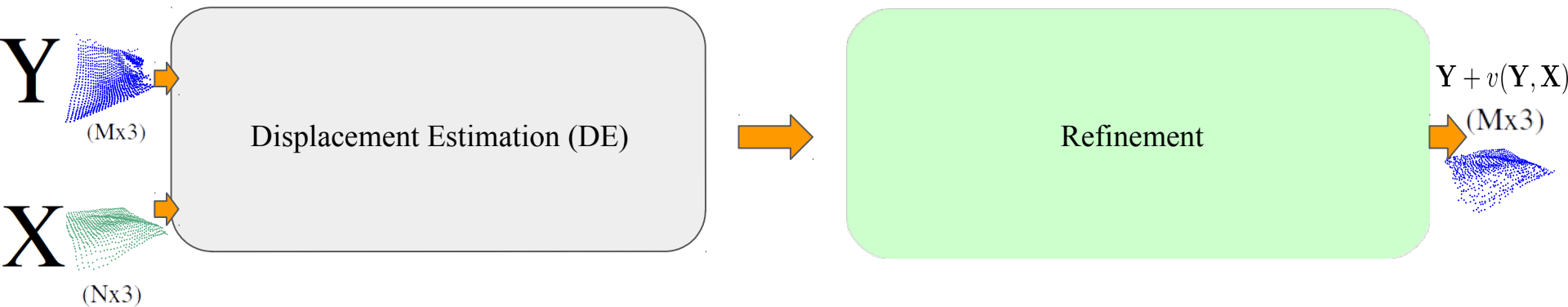
- Y: template point set, X: reference point set
- Assume M is not equal to N in general

Pipeline



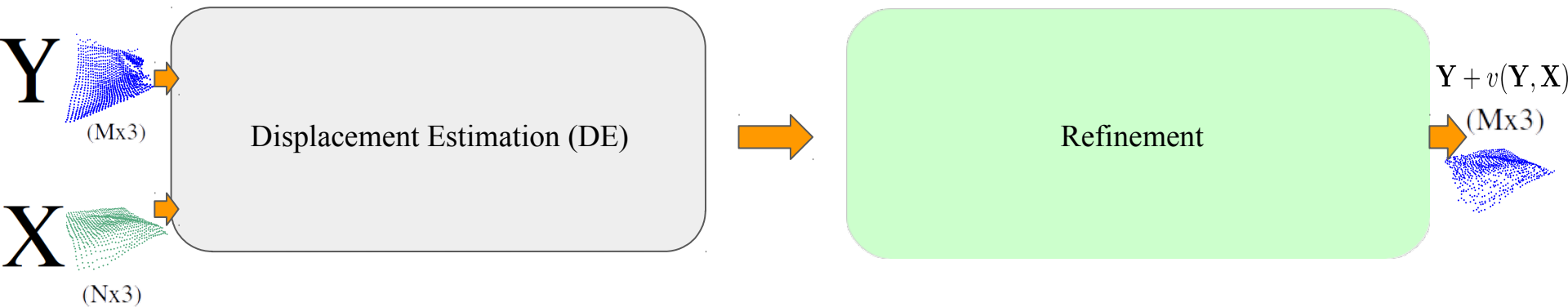
- Y : template point set, X : reference point set
- Assume M is not equal to N in general

Pipeline



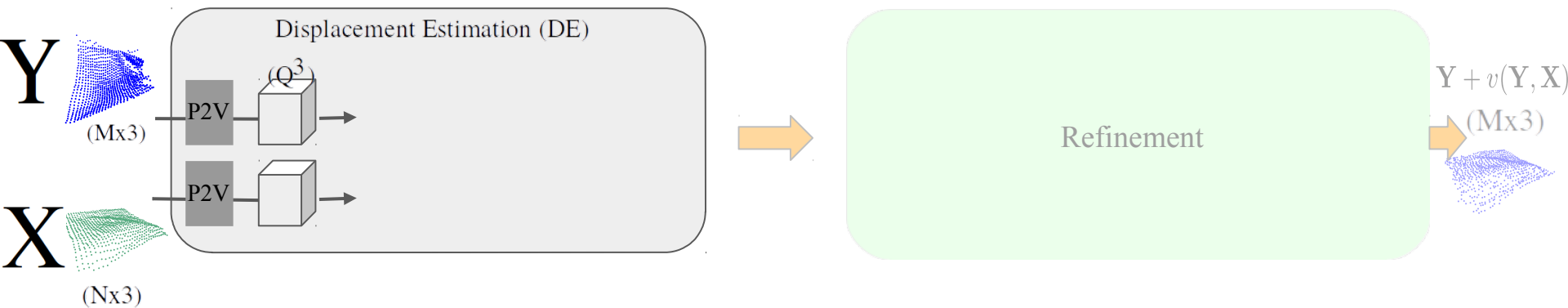
- Y : template point set, X : reference point set
- Assume M is not equal to N in general
- DE stage regresses global displacements between Y and X

Pipeline



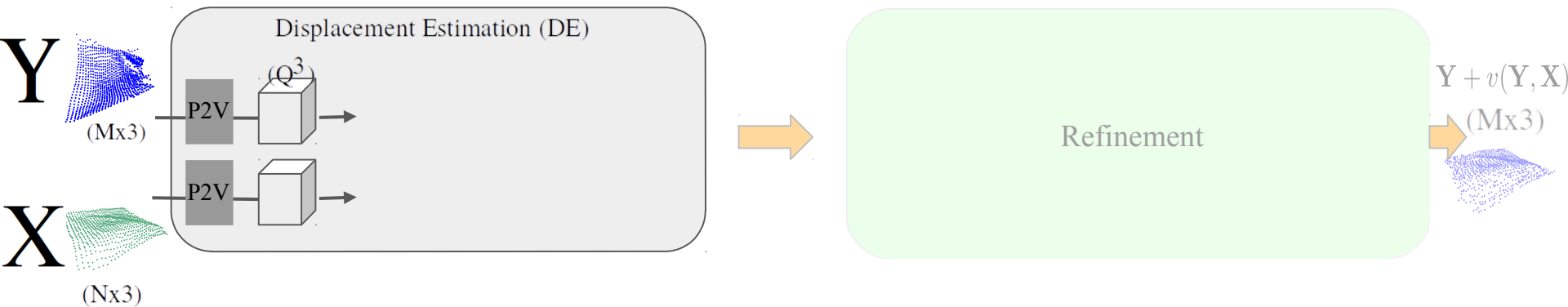
- Y : template point set, X : reference point set
- Assume M is not equal to N in general
- DE stage regresses global displacements between Y and X
- Refinement stage improves the initial displacements

Pipeline



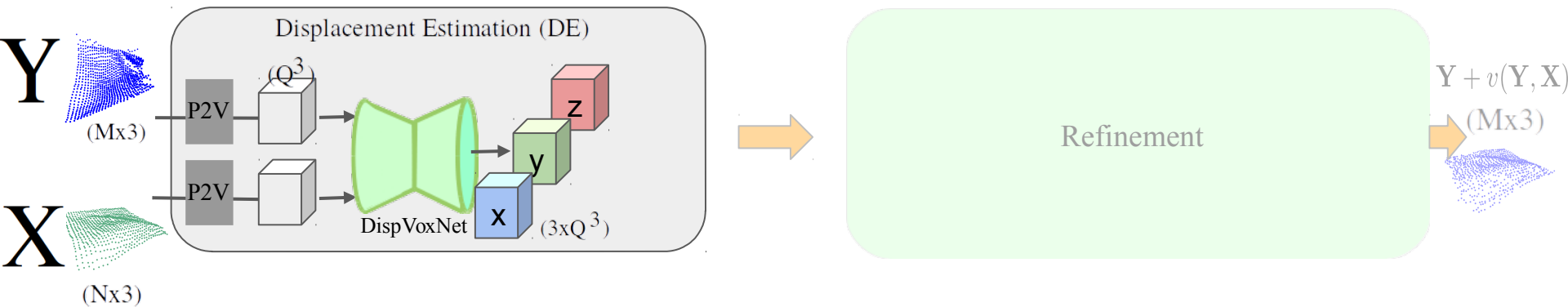
- Y and X are firstly converted into voxel representation (P2V)

Pipeline



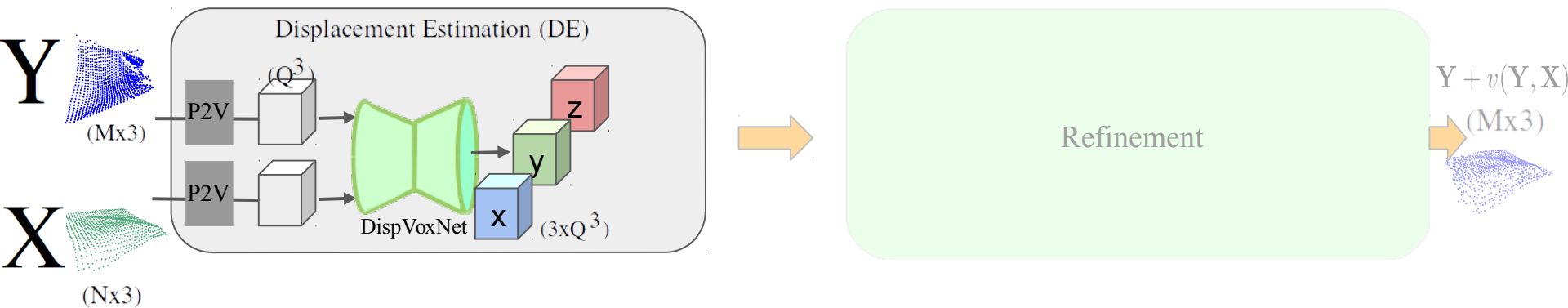
- Y and X are firstly converted into voxel representation (P2V)
- During the conversion, point-voxel correspondence information is stored in an **affinity table**

Pipeline



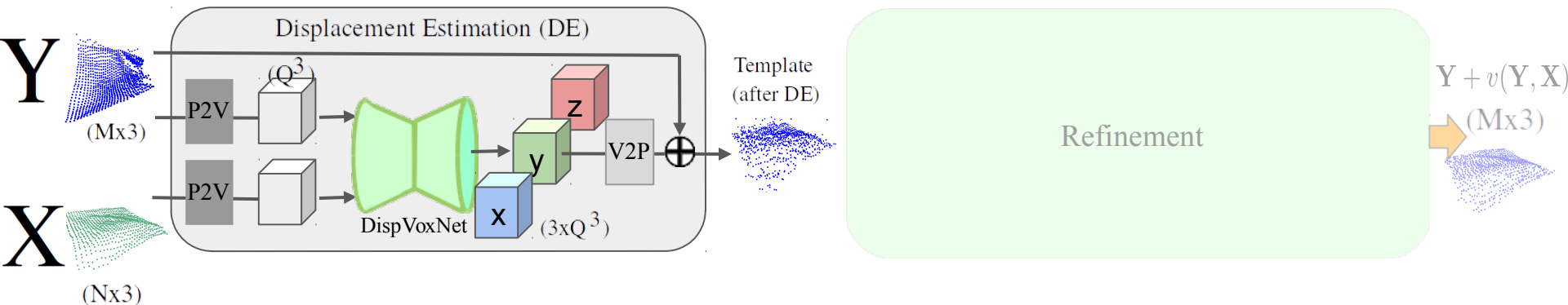
- Y and X are firstly converted into voxel representation (P2V)
- During the conversion, point-voxel correspondence information is stored in an **affinity table**

Pipeline



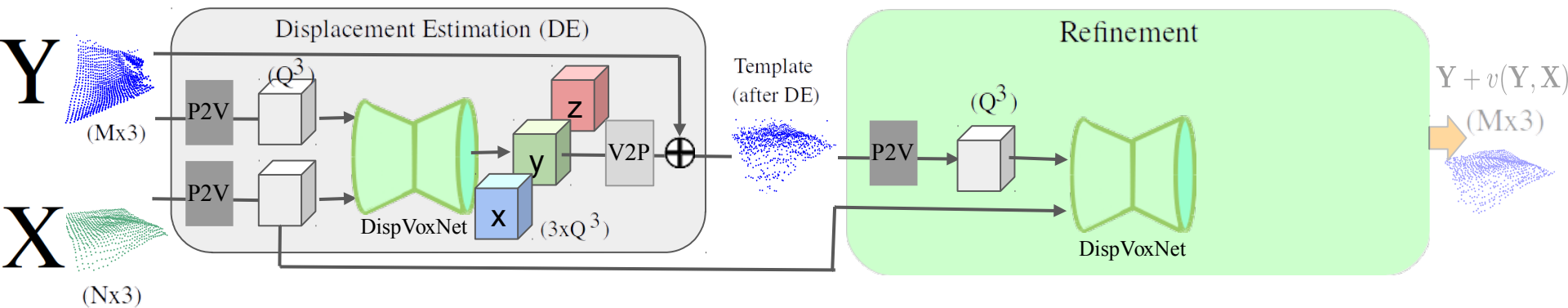
- Y and X are firstly converted into voxel representation (P2V)
- During the conversion, point-voxel correspondence information is stored in an **affinity table**
- DispVoxNet accepts two voxel grids and returns voxel displacements

Pipeline



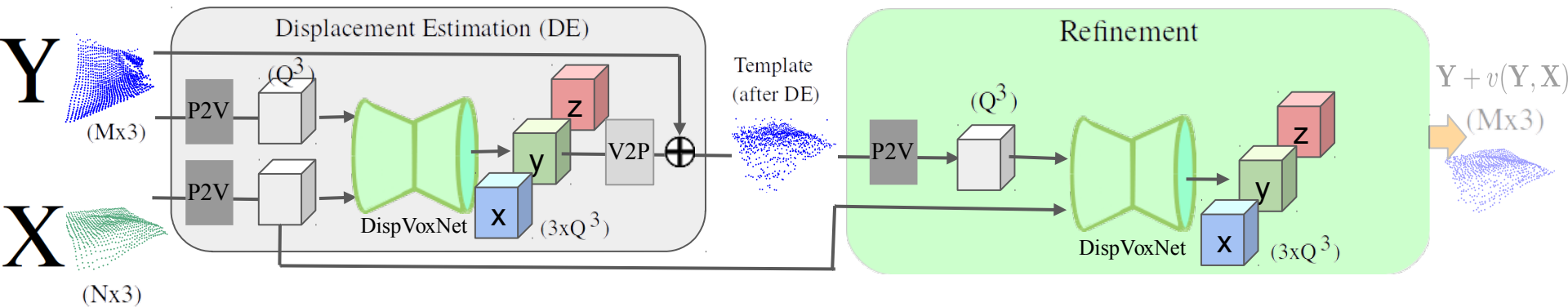
- Y and X are firstly converted into voxel representation (P2V)
- During the conversion, point-voxel correspondence information is stored in an **affinity table**
- DispVoxNet accepts two voxel grids and returns voxel displacements
- The displacements are applied using the affinity table at the end of DE stage

Pipeline



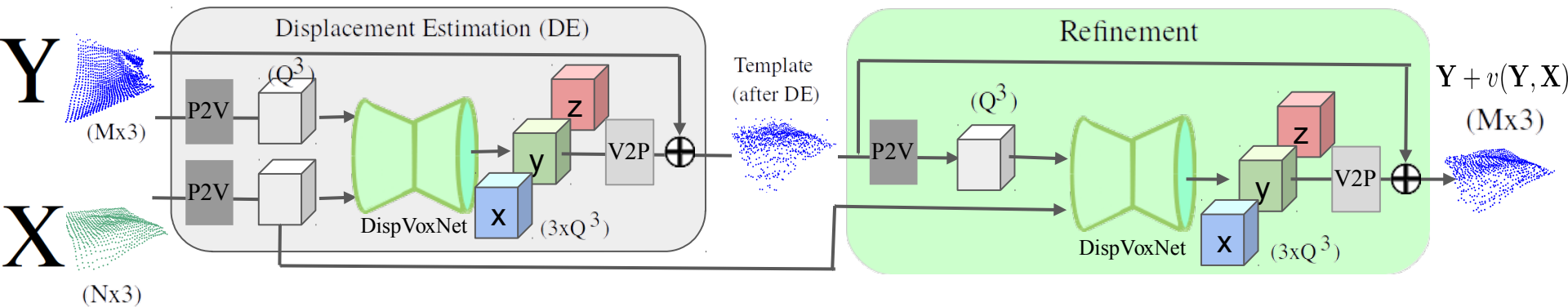
- The outputs from the DE stage are further sent to the Refinement stage after P2V

Pipeline



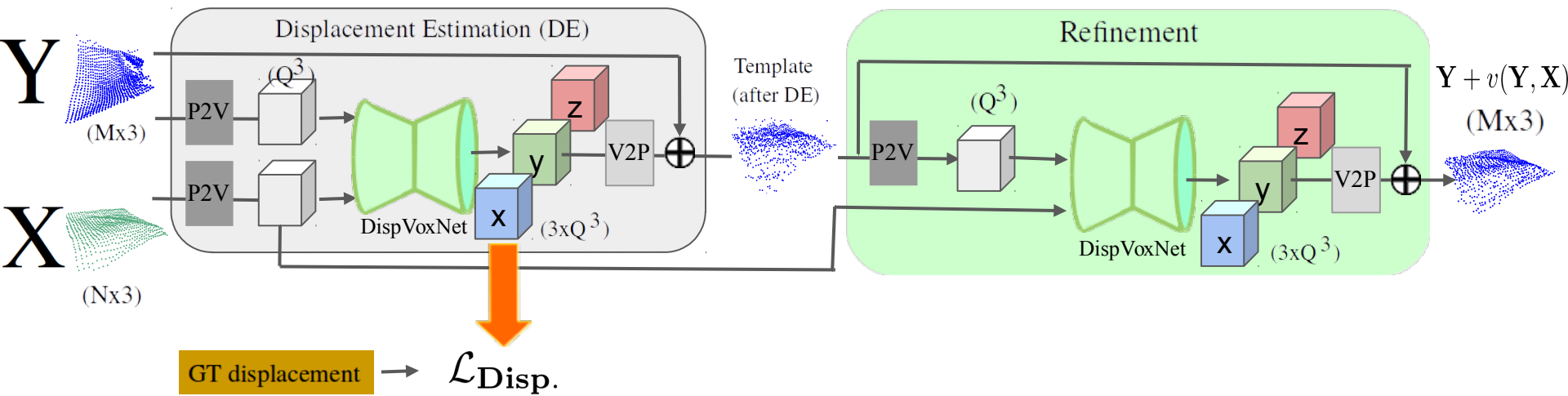
- The outputs from the DE stage are further sent to the Refinement stage after P2V
- The new instance of DispVoxNet returns small displacements for refinement

Pipeline

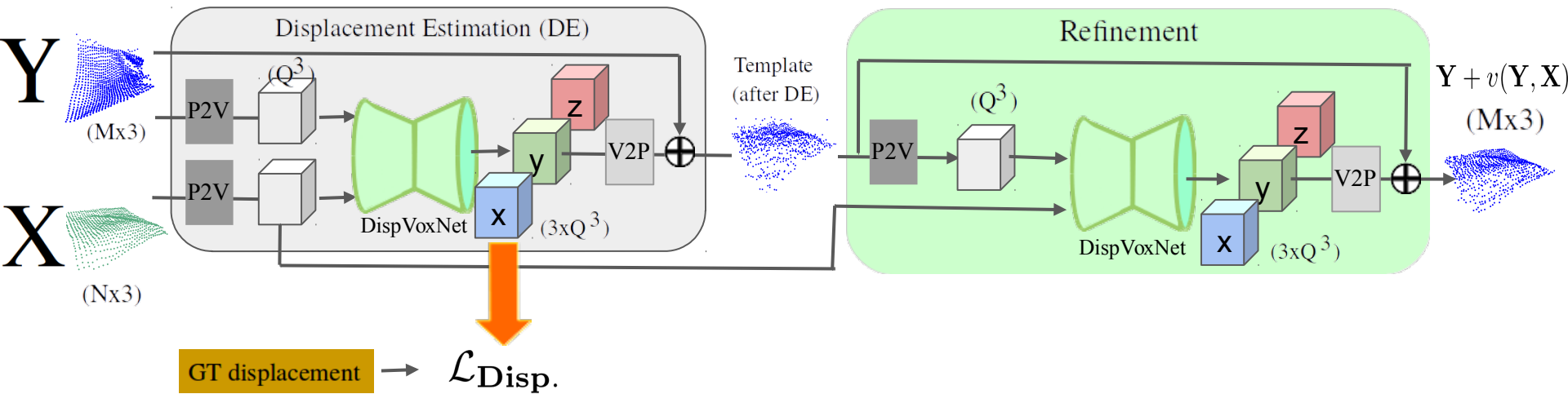


- The outputs from the DE stage are further sent to the Refinement stage after P2V
- The new instance of DispVoxNet returns small displacements for refinement
- The inferred displacements are added to the template points

Pipeline

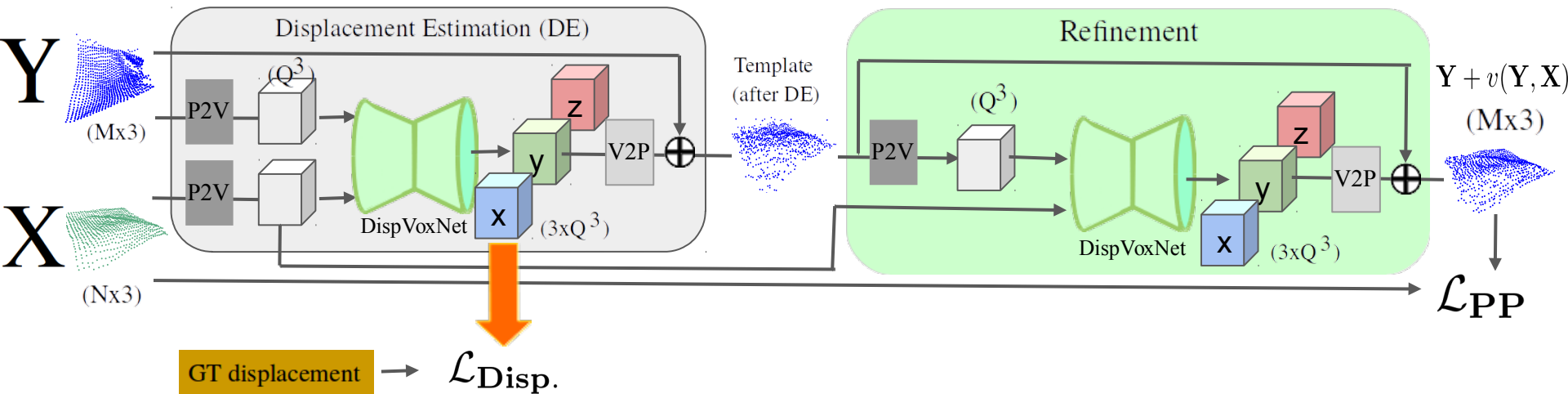


Pipeline



- The network in the DE stage is trained in a supervised manner (displacement loss)

Pipeline



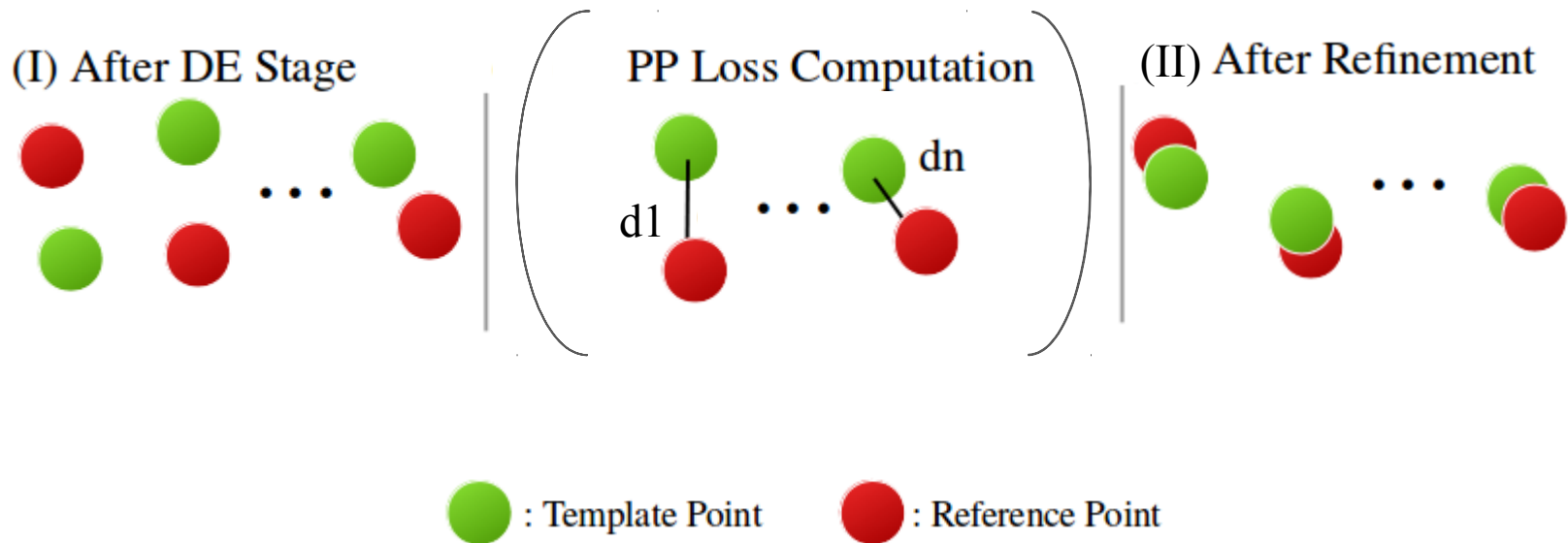
- The network in the DE stage is trained in a supervised manner (displacement loss)
- The network in the Refinement stage is trained in an unsupervised manner (point projection loss)

Loss Functions - Displacement Loss

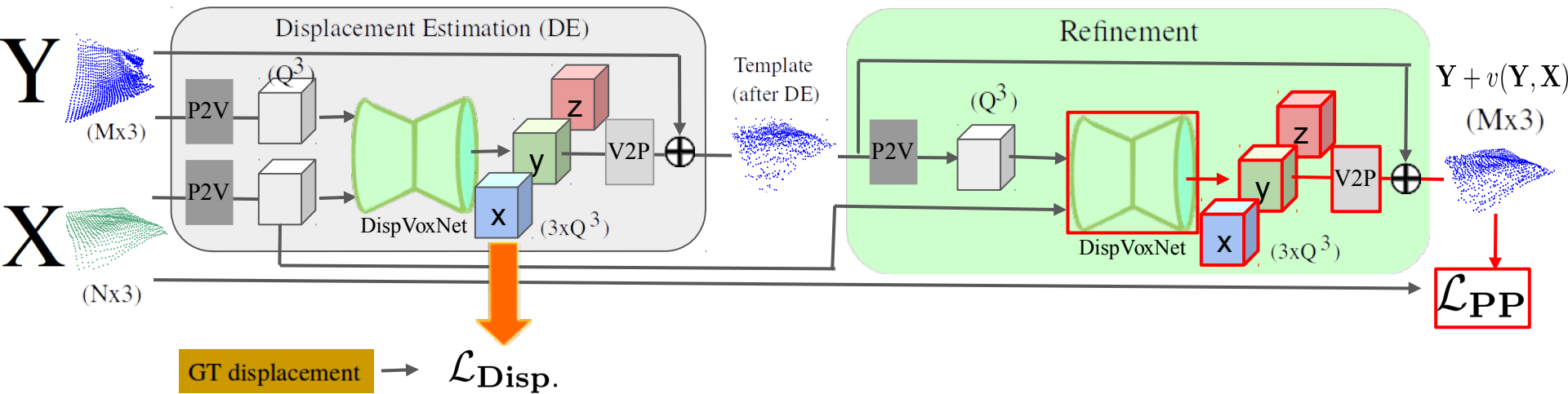
$$\mathcal{L}_{\text{Disp.}} = \left\| \begin{array}{c} \text{Network output} \\ \begin{array}{c} \text{x} \\ \text{y} \\ \text{z} \end{array} \end{array} - \begin{array}{c} \text{GT displacement} \\ \begin{array}{c} \text{x} \\ \text{y} \\ \text{z} \end{array} \end{array} \right\|_2^2$$

The diagram illustrates the Displacement Loss function. On the left, the symbol $\mathcal{L}_{\text{Disp.}}$ is followed by an equals sign. To the right of the equals sign is a large vertical double line. To the right of this line is a diagram showing two sets of three stacked cubes. The first set, labeled "Network output", consists of a blue cube labeled 'x', a green cube labeled 'y', and a red cube labeled 'z'. The second set, labeled "GT displacement", consists of a blue cube labeled 'x', a green cube labeled 'y', and a red cube labeled 'z'. A horizontal minus sign is placed between the two sets of cubes. To the right of the second set of cubes is another large vertical double line, with a '2' above it and another '2' below it, indicating the squared L2 norm.

Loss Functions - Point Projection Loss



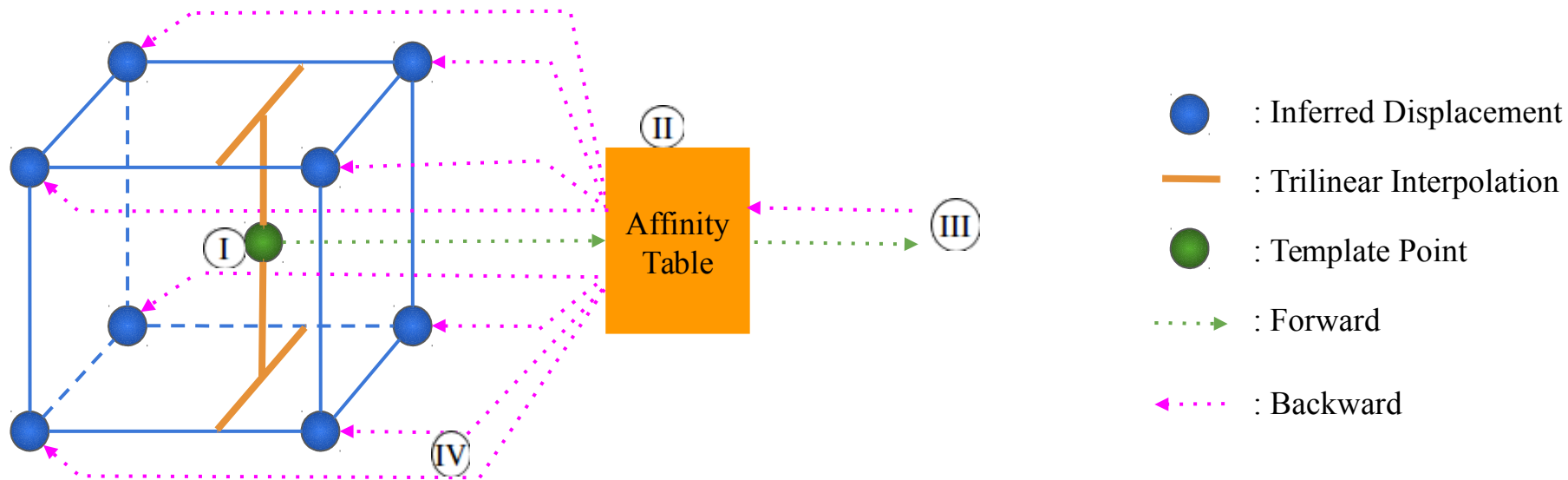
Pipeline



Problem 1: Discretisation effect due to the nature of voxel grids

Problem 2: Indifferentiability problem

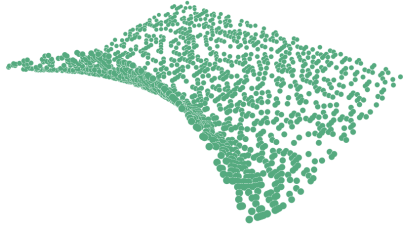
Solution for Discretisation and Indifferentiability Problems



- I. Compute trilinear weights for each template point using its 8 nearest inferred displacements
- II. Record the weights and indices of the 8 nearest displacements in the affinity table
- III. Compute the point projection loss
- IV. Distribute gradients following the IDs and weights information recorded in the affinity table in II.

Datasets

Datasets



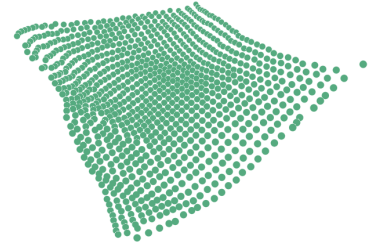
thin plate
[Golyanik *et al.* 2018]



FLAME
[Li *et al.* 2017]



DFAUST
[Bogo *et al.* 2017]



cloth
[Bednařík *et al.* 2018]

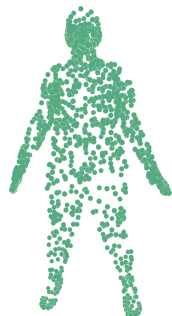
Evaluation

Quantitative Results - Baseline and Outliers

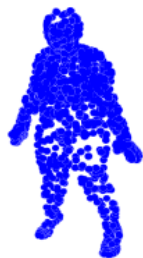
Quantitative Results - Baseline and Outliers



Template



Reference



Template



Reference

		Ours	NR-ICP [9]	CPD [38]	GMR [29]
<i>thin plate</i> [17]	<i>e</i>	0.0103	0.0402	0.0083 / 0.0192	0.2189
	σ	0.0059	0.0273	0.0102 / 0.0083	1.0121
<i>FLAME</i> [33]	<i>e</i>	0.0063	0.0588	0.0043 / 0.0094	0.0056
	σ	0.0009	0.0454	0.0008 / 0.0005	0.0007
<i>DFAUST</i> [5]	<i>e</i>	0.0166	0.0585	0.0683 / 0.0721	0.2357
	σ	0.0020	0.0215	0.0314 / 0.0258	0.8944
<i>cloth</i> [2]	<i>e</i>	0.0080	0.0225	0.0149 / 0.0138	0.2189
	σ	0.0021	0.0075	0.0066 / 0.0033	1.0121

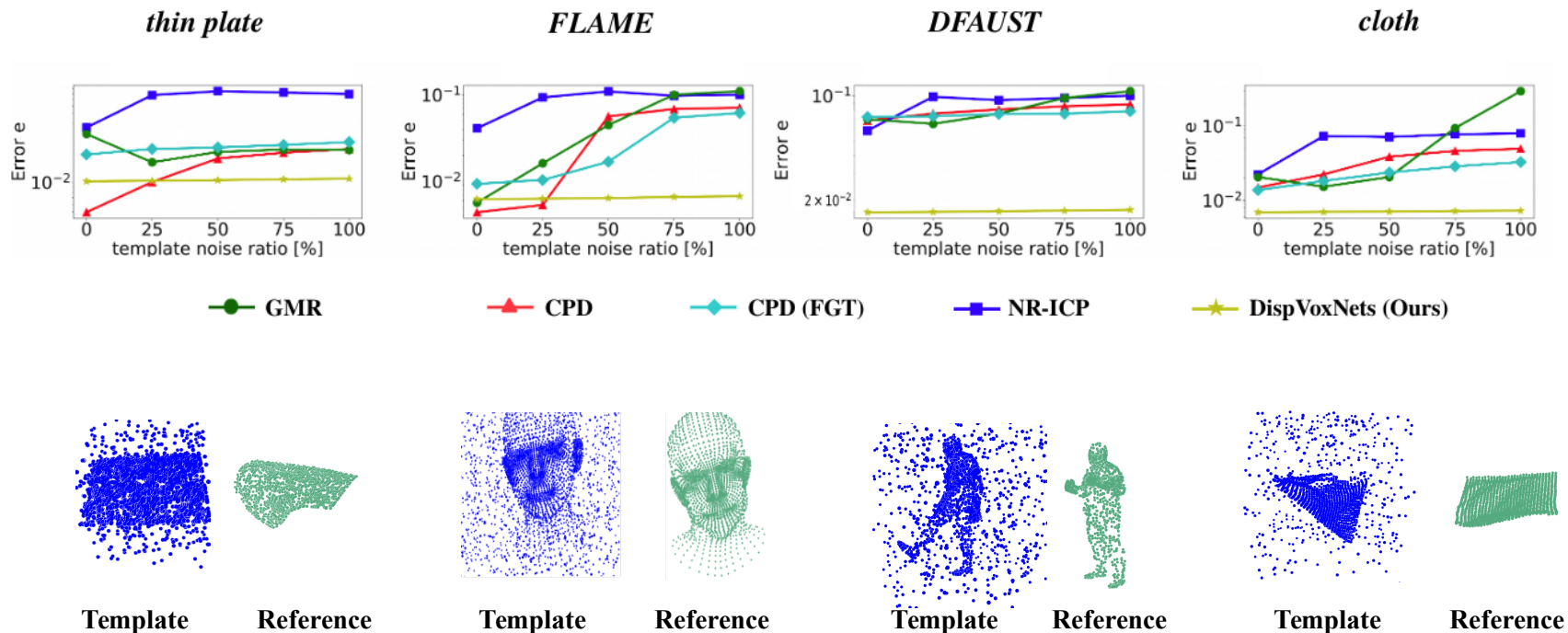
Baseline Comparison

		Ours	NR-ICP [9]	CPD [38]	GMR [29]	
<i>thin plate</i> [17]	ref.	<i>e</i>	0.0107	0.0668	0.0218 / 0.0386	0.4415
		σ	0.0061	0.0352	0.0148 / 0.0067	1.4632
	temp.	<i>e</i>	0.0108	0.0334	0.0479 / 0.0471	0.4287
		σ	0.0062	0.0281	0.0101 / 0.0038	1.3832
<i>FLAME</i> [33]	ref.	<i>e</i>	0.0084	0.0519	0.0046 / 0.0140	0.0193
		σ	0.0010	0.0451	0.0009 / 0.0006	0.0008
	temp.	<i>e</i>	0.0088	0.0215	0.0076 / 0.0201	0.0274
		σ	0.0010	0.0219	0.0010 / 0.0016	0.0019
<i>DFAUST</i> [5]	ref.	<i>e</i>	0.0167	0.0463	0.0562 / 0.0636	0.0714
		σ	0.0029	0.0195	0.0308 / 0.0216	0.0282
	temp.	<i>e</i>	0.0169	0.0426	0.0672 / 0.0710	0.0737
		σ	0.0033	0.0194	0.0291 / 0.0229	0.0243
<i>cloth</i> [2]	ref.	<i>e</i>	0.0090	0.0455	0.0248 / 0.0315	0.0288
		σ	0.0018	0.0061	0.0056 / 0.0027	0.0087
	temp.	<i>e</i>	0.0132	0.0208	0.0486 / 0.0347	0.0397
		σ	0.0019	0.0087	0.0077 / 0.0014	0.0092

Outlier

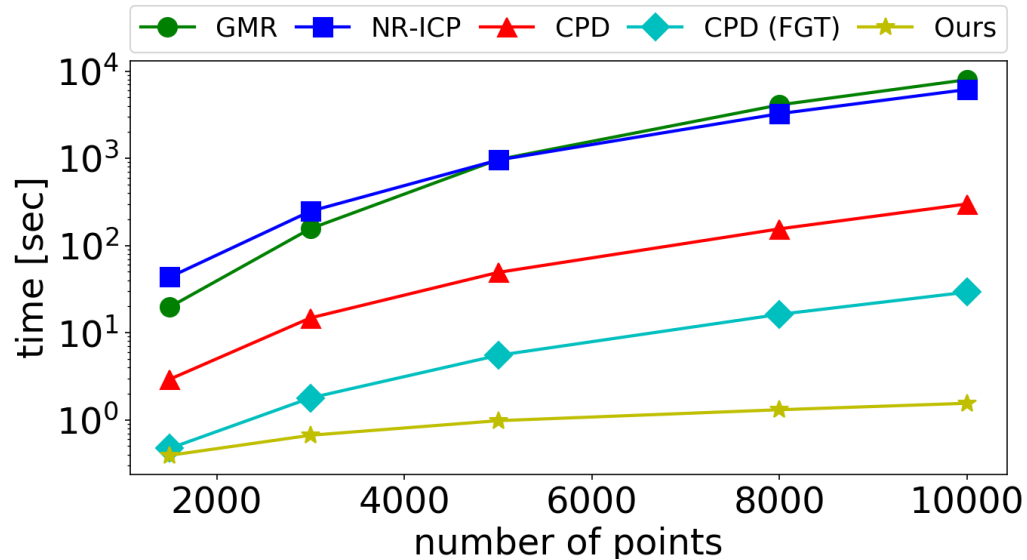
Quantitative Results - Uniform Noises

Quantitative Results - Uniform Noises



Quantitative Results - Runtime

Quantitative Results - Runtime



- With 10K points, our approach requires only a second per registration whereas others require around 2 hours - 15 seconds

Qualitative Results

Baseline Comparison

Baseline Comparison

Inputs

Template

Reference

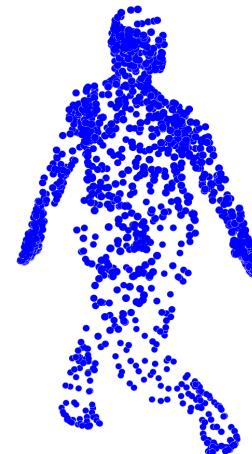
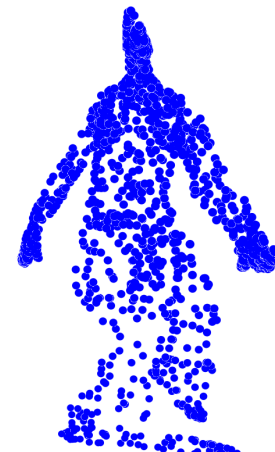
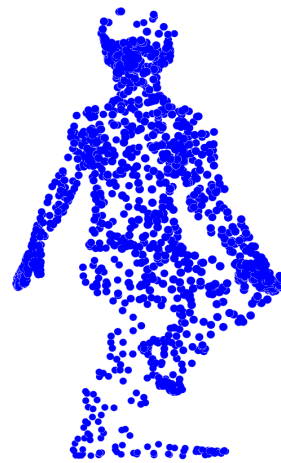
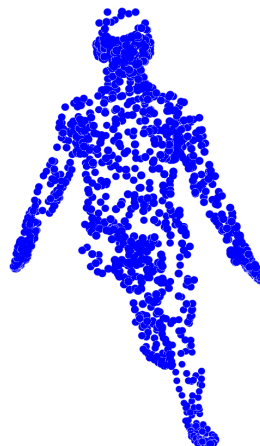
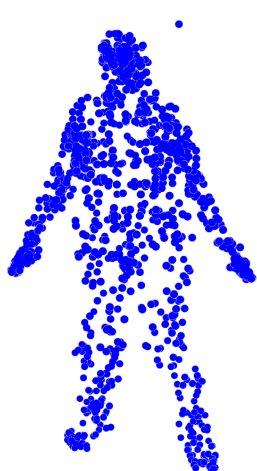
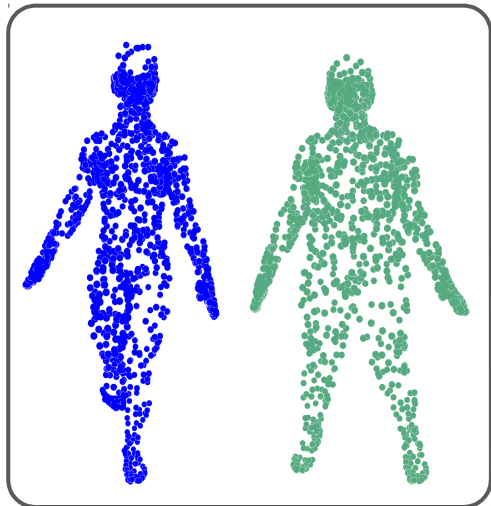
**DispVoxNets
(Ours)**

NR-ICP

CPD

CPD (FGT)

GMR



Outliers

Outliers

Inputs

Template

Reference

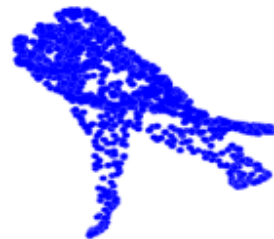
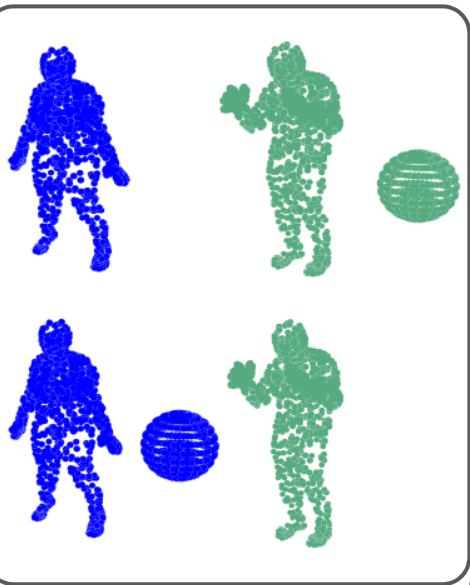
**DispVoxNets
(Ours)**

NR-ICP

CPD

CPD (FGT)

GMR



Uniform Noises

Uniform Noises

Inputs

Template

Reference

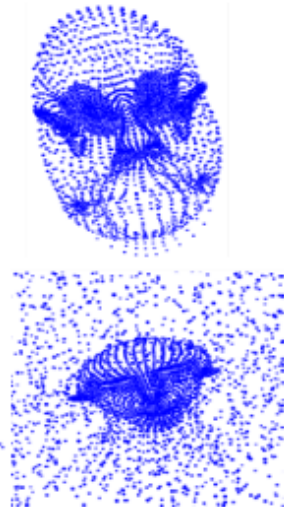
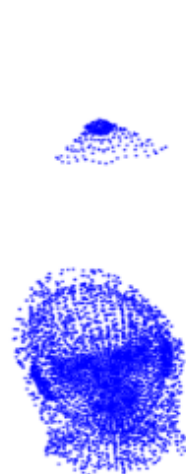
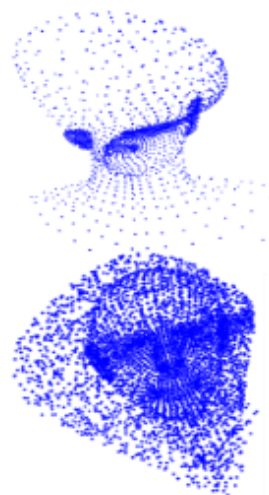
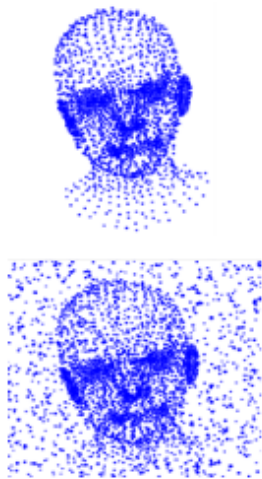
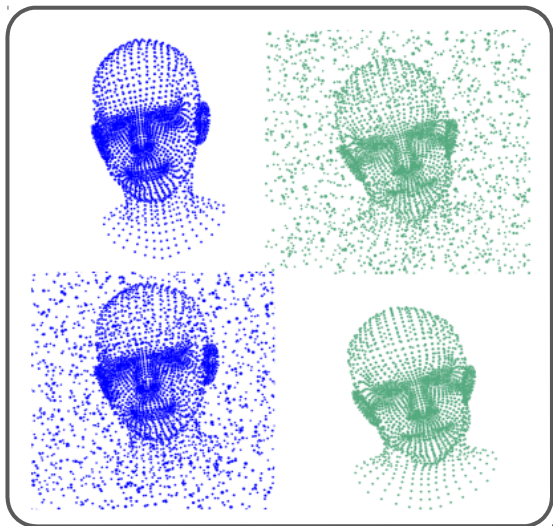
**DispVoxNets
(Ours)**

NR-ICP

CPD

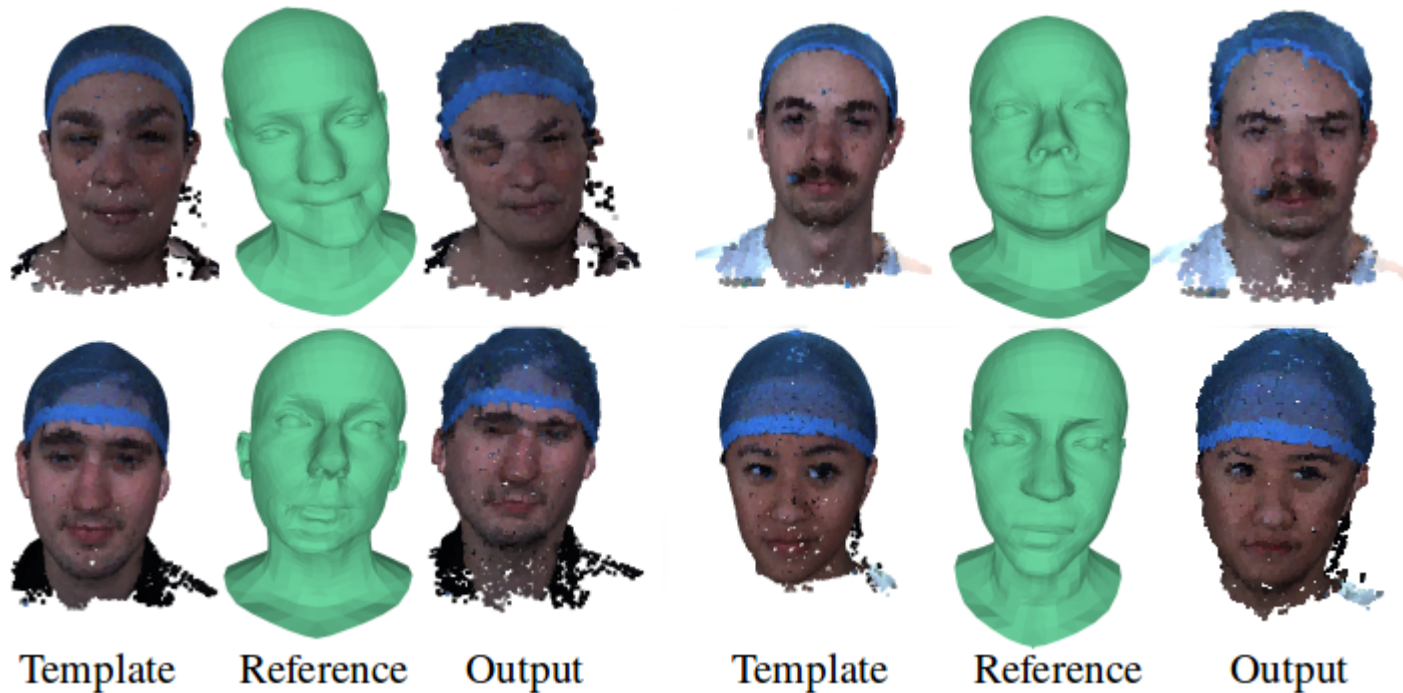
CPD (FGT)

GMR



Real Face Dataset

Real Face Dataset



Datasets: [Dai et al. 2017], [Li *et al.* 2017]

Summary

Summary

Summary

- To the best of our knowledge, this is the first neural network based approach for NRPSR that is invariant to the number and order of points.

Summary

- To the best of our knowledge, this is the first neural network based approach for NRPSR that is invariant to the number and order of points.
- Our approach outperforms other existing general-purpose methods in the presence of large deformations, articulated motion, noise, outliers and missing data.

Summary

- To the best of our knowledge, this is the first neural network based approach for NRPSR that is invariant to the number and order of points.
- Our approach outperforms other existing general-purpose methods in the presence of large deformations, articulated motion, noise, outliers and missing data.
- Runs orders of magnitude faster than previous techniques.

Summary

- To the best of our knowledge, this is the first neural network based approach for NRPSR that is invariant to the number and order of points.
- Our approach outperforms other existing general-purpose methods in the presence of large deformations, articulated motion, noise, outliers and missing data.
- Runs orders of magnitude faster than previous techniques.
- Limitation: topology preserving is not yet fully satisfying.

Summary

- To the best of our knowledge, this is the first neural network based approach for NRPSR that is invariant to the number and order of points.
- Our approach outperforms other existing general-purpose methods in the presence of large deformations, articulated motion, noise, outliers and missing data.
- Runs orders of magnitude faster than previous techniques.
- Limitation: topology preserving is not yet fully satisfying.

Project Page: <http://gvv.mpi-inf.mpg.de/projects/DispVoxNets/>

References

1. J. Bednařík, P. Fua, and M. Salzmann. Learning to reconstruct texture-less deformable surfaces from a single view. In International Conference on 3D Vision (3DV), 2018.
2. F. Bogo, J. Romero, G. Pons-Moll, and M. J. Black. Dynamic FAUST: Registering human bodies in motion. In Computer Vision and Pattern Recognition (CVPR), 2017.
3. Besl, Paul J., and Neil D. McKay. Method for registration of 3-D shapes. Sensor fusion IV: control paradigms and data structures. Vol. 1611. International Society for Optics and Photonics, 1992.
4. H. Chui and A. Rangarajan. A new point matching algorithm for non-rigid registration. In Computer Vision and Image Understanding (CVIU), 2003.
5. S. Ge, G. Fan, and M. Ding. Non-rigid point set registration with global-local topology preservation. In Computer Vision and Pattern Recognition Workshops (CVPRW), 2014.
6. S. Ge, and G. Fan. Articulated non-rigid point set registration for human pose estimation from 3D sensors. *Sensors*, 15(7), 15218-15245.
7. V. Golyanik *et al.* Extended coherent point drift algorithm with correspondence priors and optimal subsampling. In IEEE Winter Conference on Applications of Computer Vision (WACV), 2016.
8. V. Golyanik *et al.* A framework for an accurate point cloud based registration of full 3D human body scans. Fifteenth IAPR International Conference on Machine Vision Applications (MVA), 2017.
9. V. Golyanik, S. Shimada, K. Varanasi, and D. Stricker. Hdm-net: Monocular non-rigid 3d reconstruction with learned deformation model. In Virtual Reality and Augmented Reality (EuroVR), 2018.
10. B. Jian and B. C. Vemuri. A robust algorithm for point set registration using mixture of gaussians. In International Conference for Computer Vision (ICCV), 2005.
11. T. Li, T. Bolkart, M. J. Black, H. Li, and J. Romero. Learning a model of facial shape and expression from 4D scans. SIGGRAPH Asia, 2017.
12. A. Myronenko and X. Song. Point-set registration: Coherent point drift. *Transactions on Pattern Analysis and Machine Intelligence (TPAMI)*, 2010.
13. E. Smistad, et al. Medical image segmentation on GPUs—A comprehensive review. In *Medical image analysis*, 2015.
14. Z. Wang, S. Rosa, and A. Markham. Learning the intuitive physics of non-rigid object deformations. In *Neural Information Processing Systems (NIPS) Workshops*, 2018.
15. E. Tretschk, A. Tewari, M. Zollhofer, V. Golyanik, and C. Theobalt. DEMEA: Deep Mesh Autoencoders for NonRigidly Deforming Objects. *arXiv e-prints*, 2019.
16. H. Dai, N. Pears, W. A. P. Smith, and C. Duncan. A 3d morphable model of craniofacial shape and texture variation. In ICCV, 2017.

Questions?

DispVoxNets: Non-Rigid Point Set Alignment with Supervised Learning Proxies

Soshi Shimada^{1,2}

Vladislav Golyanik³

Edgar Tretschk³

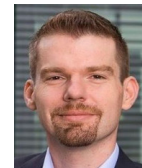
Didier Stricker^{1,2}

Christian Theobalt³

¹University of Kaiserslautern

²DFKI

³MPI for Informatics, SIC



Thank you